# ARTICLES

## Assembly of *p*-Nitroaniline Molecule in the Channel of Zeolite MFI Large Single Crystal for NLO Material

**Feifei Gao,† Guangshan Zhu,† Yue Chen,† Yi Li,† and Shilun Qiu*,†**

*State Key Lab of Inorganic Synthesis and Preparative Chemistry, Department of Chemistry, Jilin University, 119 Jiefang Road, Changchun 130023, P. R. China*

*Received: August 6, 2003; In Final Form: November 21, 2003*

A large high-quality zeolite MFI single crystal 3.0 × 1.5 × 1.5 $mm^3$ in size was synthesized by means of a nutrition supplemental method and a *p*-nitroaniline (PNA)/MFI single crystal was prepared via physical vapor deposition. The light yellow PNA/MFI single crystal changed to green when irradiated by 1062 nm fundamental wavelength from a Nd:YAG pulse laser, and the transmitted light includes the SHG wavelength 527 nm. Both C−H−N analysis and molecular mechanics suggested that there were five PNA molecules encapsulated in each MFI unit cell, and the structure of the PNA molecule within the MFI microporous system is noncentrosymmetric. The PNA/MFI single crystal would be potentially applied as a NLO material.

### Introduction

Being one of the most important second-order nonlinear optical (NLO) properties, second harmonic generation (SHG) has been extensively studied for the design, the characterization, and the application of NLO materials. Organic materials with NLO properties are usually investigated as electric field-poled polymers and acentric Langmuir−Blodgett and self-assembled multilayer thin films, due to their better properties: short response time, large nonlinear optical susceptibility, etc.[1−5] However, the most applications of NLO materials are based on inorganic compounds, such as KDP ($KH_2PO_4$), KTP ($KTiOPO_4$), and LBO ($LiB_3O_5$), because organic crystals exist many shortcomings compared with inorganic materials, for example, the poor mechanical capability, the low melting point and rigidity, the easy deliquescence, and the high decomposability.

It was known that the *p*-nitroaniline (PNA) molecule showed significant NLO property; however, there is no SHG from the PNA organic crystal due to its centrosymmetric structure,[6−8] which is a challenging obstacle for the application of such material. To construct a new functional material with optical properties, scientists have made many attempts,[9−11] one of which is the encapsulation of a functional material in the channels or cavities of zeolites. Owing to their uniform pore size and significant pore volume, zeolites and molecular sieves are widely used as a host for optoelectronic devices, nonlinear optics, selective sensors, and zeolite−polymer composites. The functional molecule/zeolite composites exhibit potential chemical and physical characters, including optical, electric, and magnetic properties, according to their new structures.[12,13] Ozin and co-workers reported that the cavities or channels in zeolites provided excellent coordinate environments toward the guests encapsulated (e.g., the supercages of the zeolite Y host), which created guest−host inclusion compounds with wide application in material research of nonlinear optics and photonic.[14] The generation of numerous clusters and superclusters (cluster arrays) assembled in the channels of zeolite LTL has been approached by means of the "ship-in-a-bottle" method.[15] Alkali metal clusters generated in the cage of zeolite LTA and the channel of zeolite MOR exhibit interesting phenomena in optical properties as well as magnetic ones.[16] Strong visible photoluminescence from boron nitride nanoparticles encapsulated in zeolite MFI by means of chemical vapor deposition was reported.[17] Notably, the hosts mentioned above are based on zeolite powders. Such a defect limits their application in optoelectronic microdevices, so many an effort has been made to synthesize large high-quality single crystals of zeolites, which are used as hosts for the preparation of molecule/zeolite composites. Schüth and co-workers reported the linear alignment of a laser dye in the channels of high optical quality APO-5 (AFI) crystals of about 0.5 mm in length, which showed new spectroscopic properties and laser action in the host−guest system.[12,13] We have reported the synthesis of large zeolite MFI single crystals with a monocrystalline silicon slice (MSS) as the silicon source and the preparation of Si nanoparticles in a large MFI single crystal, from which strong visible photoluminescence (PL) at both room temperature and 10 K were observed.[18]

In this work, by means of a nutrition supplemental method, a larger high-quality MFI single crystal with the average size of 3.0 × 1.5 × 1.5 $mm^3$ was synthesized as the host material, and the SHG-active PNA/MFI single crystal was prepared via physical vapor deposition (PVD). The second harmonic generation from PNA/MFI crystal was characterized, and the structure of PNA molecules inside the channel of the MFI framework was simulated by means of molecular mechanics.

* Corresponding authors. S.Q.: Fax:+86-431-5671974. E-mail: sqiu@mail.jlu.edu.cn.
† Jilin University.

10.1021/jp036330y CCC: $27.50 
Published on Web 02/25/2004

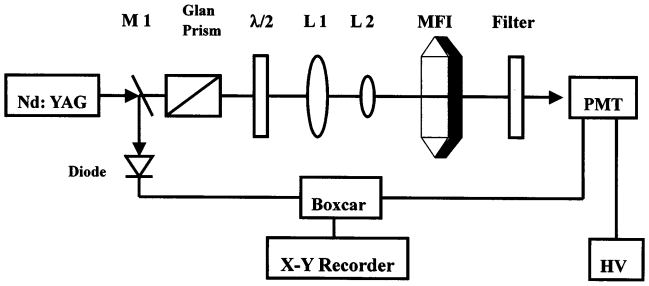


**Figure 1.** Experimental setup for second harmonic generation measurement of PNA/MFI single crystal.

## Experimental Section

A high-quality large single crystal of MFI was synthesized with a nutrition supplemental method based on our previous work.[18] A thin piece of polished monocrystalline silicon (0.40 g, $10 \times 10 \times 0.5$ mm$^3$) was placed into a Teflon-lined stainless steel autoclave together with 10 mL of reaction mixture with the molar ratio 10.5 HF:7.0 TPAOH:900 $H_2O$. The crystallization was carried out at 180 °C. Three days later, the autoclave was taken out of the oven and cooled to room temperature. A supplemental solution of TPAOH was then added into the above crystallization system to adjust the pH value to 5.5. The autoclave was sealed again and the crystallization was resumed. Such a supplemental procedure was repeated twice during the whole crystallization process, which lasted for 18 days. The calcination of large MFI single crystals was carried out under an $O_2$ atmosphere. The temperature was ramped at 1 °C min$^{-1}$ to 150 °C, maintained at this temperature for 5 h, then increased to 550 °C at a rate of 0.5 °C min$^{-1}$, and kept at 550 °C for over 40 h. The PNA-encapsulated zeolite MFI composite single crystal was prepared by physical vapor deposition (PVD). The calcined large MFI single crystal was kept in the vacuum chamber (background pressure was less than $10^{-3}$ Torr) together with PNA. The temperature was increased from room temperature to 150 °C at a rate of 1 °C min$^{-1}$, and kept at 150 °C for 3 h. The product was then cooled in the vacuum chamber gradually, and washed by ethanol; a bright yellow PNA/MFI single crystal was obtained.

## Product Analysis

The morphology of MFI large single crystals was observed by a Leica polarizing microscope. The XRD was performed by a Siemens D5005 diffractometer using Cu K$\alpha$ radiation, 40 kV, 35 mA, with a scanning rate of 0.2° min$^{-1}$ ($2\theta$). $N_2$ adsorption measurements were conducted on an ASAP 2010M porosimeter at 77 K. TGA and DTA were performed on a Netzsch STA 449c thermogravimetric and differential thermal analyzer, under a flow of $N_2$ atmosphere at a heating rate of 20.0 °C min$^{-1}$ from 50 to 700 °C. The FT-IR spectra were collected on a Nicolet Impact 410 FTIR in the range 400−4000 cm$^{-1}$ by using the KBr disk method. Before FT-IR measurements, the samples of PNA, PNA/MFI crystal, and MFI crystal were ground to fine powder. The Raman spectra were performed on a Bruker FT-IR Roman instrument, with laser line 1064 nm, power 60 mV, and scanning 100 times. To measure the sample of PNA/MFI crystal, the *b* axis of the PNA/MFI crystal was aligned to parallel to the Raman laser beam. The C−H−N data of the samples were determined by the results of inductively coupled plasma (ICP, Perkin-Elmer 3300DV) and chemical analysis.

The second harmonic generation measurement experimental arrangement was shown schematically in Figure 1. A Nd:YAG laser ($\lambda = 1064$ nm) was used as the pump light, with pulse width 10 ns and repeat rate 10 Hz. After passing the Glan prism and $\lambda/2$ wave plate, the light was aligned and focused onto a PNA/MFI single crystal with an angle of incidence of 90°. The intensity of second harmonic generation was detected with a photomultiplier tube (PMT) and processed with a boxcar integrator. The signal was recorded on an X−Y recorder. A single crystalline quartz with $d_{11} = 0.46$ pm/V was used as a reference.

The molecular modeling was carried out by using the Cerius$^2$ (version 4.6) software package developed by Accelrys Inc. The whole procedure consists of two steps. The first step involves the location of PNA molecules in MFI framework through the rapid Monte Carlo method;[19−21] the second step is to obtain the accurate configuration of PNA molecules and the energy of the system by molecular mechanical energy optimization. The force constants used in both steps are derived from the Burchart1.01-Dreiding2.21[22,23] force field.

In the Monte Carlo simulation, the zeolite framework was assumed to be fixed and the PNA molecule was assumed to be rigid and to move randomly. The Monte Carlo simulation was carried out in canonical ensemble at 300 K using the conventional Metropolis[24] algorithm based on the configurational energy change: $P = \min[1;\exp(-\Delta E/kT)]$, where $P$ is the probability of the move being accepted, $\Delta E$ is the energy change between the new configuration and the previous configuration, $k$ is the Boltzmann constant, and $T$ is the temperature of the simulation. If the change in energy ($-\Delta E$) resulting from the move of the PNA molecules was negative, the Boltzmann factor ($\exp(-\Delta E/kT)$) was computed and compared to a randomly generated number between zero and one. If the random number was less than the Bolzmann factor, the move of the PNA molecules was selected; otherwise, it was rejected. Twelve Monte Carlo runs were performed with different number of PNA molecules located in one unit cell of the MFI framework. Each Monte Carlo run took 100 000 steps, and the models with the lowest energies in each run would be saved.

In the energy optimization step, the twelve models with the lowest energies were studied. The MFI framework was still assumed to be fixed while the PNA molecules were relaxed. In this procedure, the location and the configuration of PNA molecules were further modified. After the energy optimization was done, the nonbonding interaction energies including van der Waals energies ($E_V$) and hydrogen bonding energies ($E_H$) between the PNA molecule and MFI framework, and inter-PNA molecules were calculated.

## Results and Discussion

In our previous work,[18] a large zeolite MFI single crystal $2 \times 1 \times 1$ mm$^3$ in size was synthesized. Because the silica source, a monocrystalline silicon slice, is superfluous and HF plays the role of mineralizer, the only consumed nutrition in the reaction solution is TPAOH. If consumed TPAOH was supplied during the crystallization procedure, a larger MFI single crystal would be expected. In this work, when the nutrition supplemental method described above was utilized during the crystallization procedure, a larger MFI single crystal $3 \times 1.5 \times 1.5$ mm$^3$ in size was synthesized. Under a polarizing microscope, the MFI crystals are transparent single crystals without twinning and with good morphology and large size, photographs of which are shown in Figure 2. If a TPAOH supplemental solution was added after crystallization time and prolonged the crystallization time, a larger but opaque MFI crystal was obtained.

The TG-DTA plots of as-synthesized samples, and the nitrogen isothermal adsorption of calcined sample suggest that the channels of the large MFI single crystals are open without


**Figure 2.** Photograph of MFI single crystals under polarizing microscope.

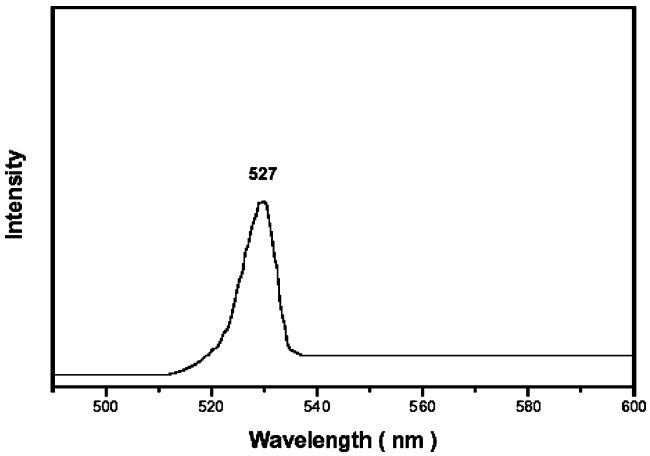


**Figure 3.** Emission of PNA/MFI single crystal under a Nd:YAG pulse laser of 1064 nm.

blocking and with good qualification for the encapsulation of PNA molecules. Owing to their special structure of straight channels with pore size 0.53 × 0.56 $nm^2$, which interconnect the zigzag channels with pore size 0.51 × 0.55 $nm^2$, zeolite MFI crystals are suitable for the encapsulation of PNA molecules (with the size of about 0.47 × 0.73 $nm^2$), and the preparation of PNA/MFI single crystals. The second harmonic can be generated from a PNA/MFI single crystal irradiated by the 1064 nm fundamental wavelength from a Nd:YAG pulse laser, and the transmitted light includes the SHG wavelength 527 nm (Figure 3). The photograph of the green PNA/MFI single crystal under the laser is shown in Figure 4, which suggests that the PNA/MFI single crystal is SHG active.

Figure 5 is the XRD patterns of (a) PNA/MFI crystal, (b) MFI crystal, (c) mechanically ground PNA + MFI mixture, and (d) PNA. Due to the sample of a mechanically ground PNA + MFI mixture containing both PNA and MFI crystals, the pattern of a mechanically ground PNA + MFI mixture (Figure 5c) presents both PNA and MFI characteristic peaks (Figure 5b and 5d). The pattern of the PNA/MFI crystal (Figure 5a) does not show any characteristic peaks of PNA. It indicates that there is no PNA outside the MFI single crystals. The PNA molecules were encapsulated inside the MFI channels.

In the IR spectra (Figure 6), the peaks at 3510 and 3412 $cm^{-1}$ (due to the N—H asymmetric stretching and symmetric stretching), the peaks at 1627 and 1599 $cm^{-1}$ (due to C═C phenyl framework vibrations), and the peaks at 1500 and 1313 $cm^{-1}$ (due to asymmetric $NO_2$ stretching and symmetric $NO_2$ stretching)[25] in the spectrum of ground PNA/MFI (Figure 6b) cannot

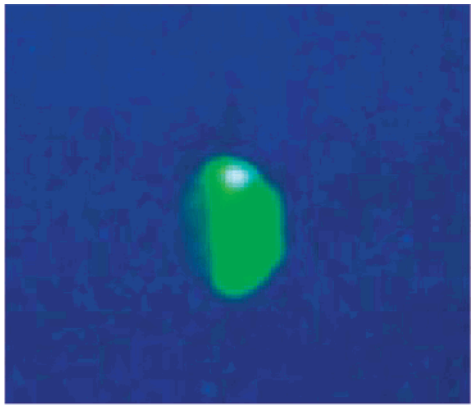

**Figure 4.** Photograph of PNA/MFI single crystal under the 1064 nm fundamental wavelength from a Nd:YAG pulse laser.

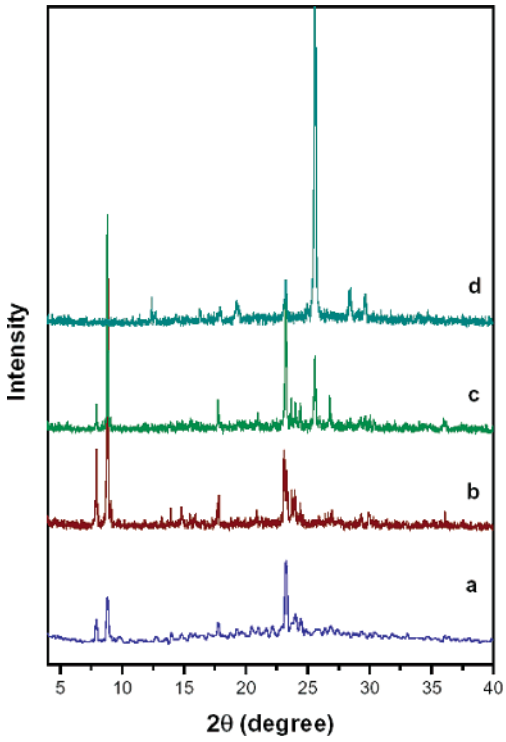


**Figure 5.** XRD patterns of (a) PNA/MFI crystal, (b) MFI crystal, (c) mechanically ground MFI + PNA mixture, and (d) PNA.

be found in the spectrum of MFI (Figure 6c) but can correspondingly be observed in the spectrum of PNA (Figure 6a). Notably, the two N—H stretching peaks of PNA at 3477 and 3361 $cm^{-1}$ have shifted to higher wavenumbers 3510 and 3412 $cm^{-1}$, respectively, in the spectrum of ground PNA/MFI (Figure 6b), which is because the N—H···O hydrogen bonds between PNA molecules in the PNA crystal are broken when the PNA molecule is dispersed in the channel of the MFI crystal. There is little difference between the phenyl framework vibrational peaks in the IR spectra of the PNA crystal (Figure 6a) and ground PNA/MFI (Figure 6b). Meanwhile, for the Raman spectra (Figure 7), the strong peaks at 1286 $cm^{-1}$ in the spectra of both PNA (Figure 7a) and mechanically ground MFI + PNA mixture (Figure 7b) disappear in the spectrum of the PNA/MFI single crystal, while the peak at 1316 $cm^{-1}$ in the spectrum of the PNA/MFI single crystal (Figure 7c) obviously strengthens. In the PNA crystal, most PNA molecules are hydrogen-bonded, which causes the shift of the $NO_2$ symmetric stretching (located at 1357−1318 $cm^{-1}$ in Ar—$NO_2$[26,27]) from 1316 to 1286 $cm^{-1}$. But a weak peak at 1316 $cm^{-1}$ still exists in the spectrum of

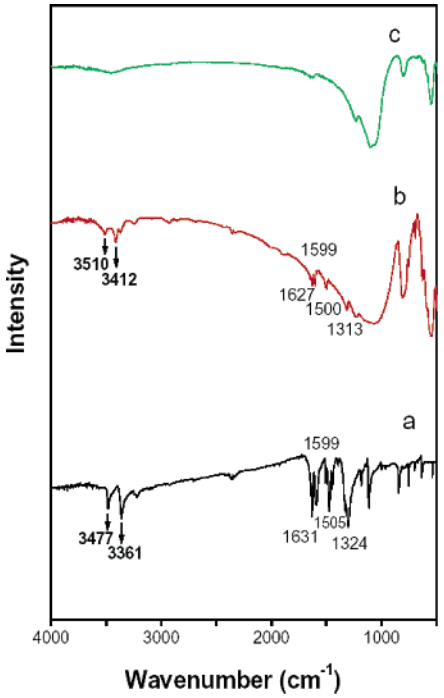


**Figure 6.** IR spectra of (a) PNA, (b) ground PNA/MFI, and (c) ground MFI.

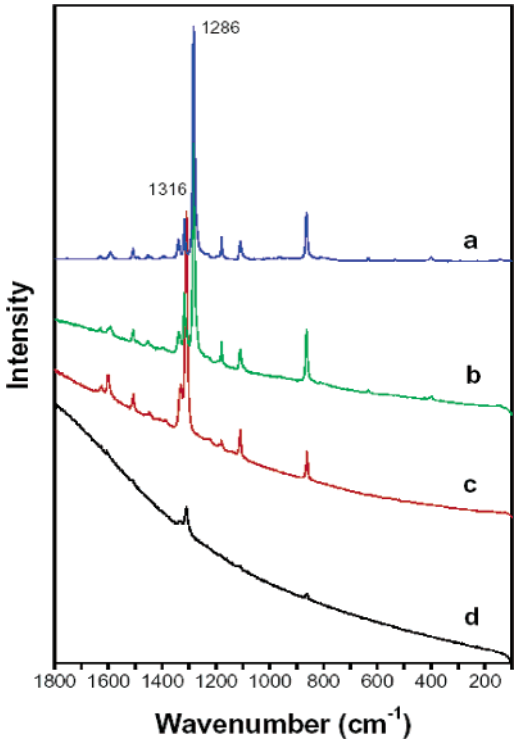


**Figure 7.** Raman spectra of (a) PNA, (b) mechanically ground PNA + MFI mixture, (c) PNA/MFI crystal, and (d) mechanically ground PNA/MFI.

PNA (Figure 7a) due to the few terminals Ar−$NO_2$ on the surface of the PNA crystal. When PNA molecules are dispersed into MFI channels, the hydrogen bonds are broken; therefore the peak at 1286 $cm^{-1}$ disappears while the peak at 1316 $cm^{-1}$ strengthens. The results of both the IR and the Raman spectra suggest that PNA molecules have been encapsulated in the channels of MFI crystal and exist as single molecules.

On the basis of the results of C−H−N analysis (C = 5.07 wt %, H = 0.48 wt %, and N = 1.48 wt %), the number of

**TABLE 1: Nonbonding Interaction Energies ($E_{inter}$) Including Van der Waals Energies ($E_V$) and Hydrogen Bonding Energies ($E_H$) between PNA Molecule and MFI Framework and between PNA Molecules**

| no. of PNA[a] | $E_V$ (kcal·mol$^{-1}$) | $E_H$ (kcal·mol$^{-1}$) | $E_{inter}$ (kcal·mol$^{-1}$) |
|---|---|---|---|
| 2 | −12.58 | −0.27 | −12.85 |
| 3 | −13.65 | −2.16 | −15.81 |
| 4 | −16.48 | 0 | −16.48 |
| 5 | −18.55 | 0 | −18.55 |
| 6 | −1.88 | −2.15 | −4.03 |
| 7 | 0.01 | 0 | 0.01 |
| 8 | 4.19 | −12.40 | −8.3 |
| 9 | 11.67 | −11.34 | 0.33 |
| 10 | 64.62 | −13.92 | 50.7 |
| 11 | 158.34 | −12.57 | 145.77 |
| 12 | 252.14 | −13.24 | 238.9 |
| 13 | 453.60 | −5.00 | 448.6 |

[a] The number of PNA in a MFI unit cell.

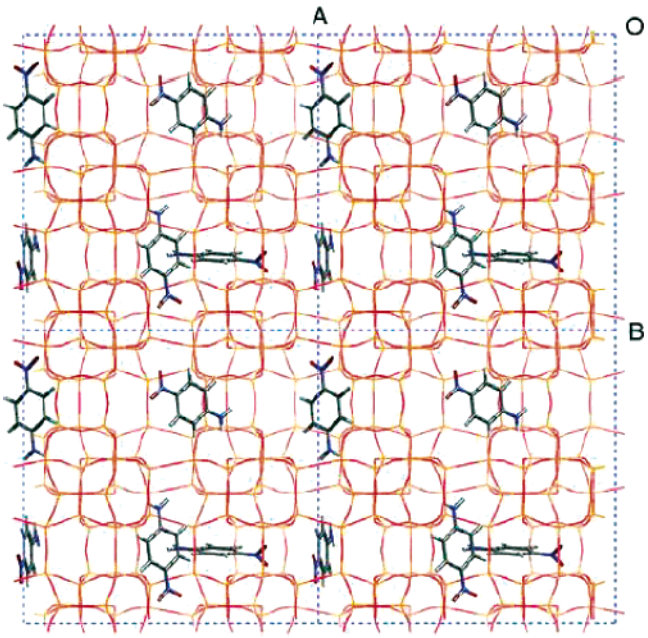


**Figure 8.** Most suitable configuration of PNA molecule in the channel of MFI framework along the [001] direction.

PNA molecules in each MFI unit cell was calculated to be 5. The position of PNA molecules in MFI crystal unit cells was also investigated by means of molecular mechanics. The nonbonding interaction energies ($E_{inter}$), including van der Waals energies ($E_V$), and the hydrogen-bonding energies ($E_H$) between PNA molecule and the MFI framework and between PNA molecules are listed in Table 1. It shows that the nonbonding interaction energy was lowest when 5 PNA molecules are kept in a MFI unit cell, which fits well with the C−H−N analysis. The most suitable molecular configuration of PNA in the channel of MFI is shown in Figure 8. In the configuration, there is a hydrogen bond neither between the PNA molecule and MFI framework nor between PNA molecules. It agrees well with both the IR and the Raman results. The configuration also shows that the structure of PNA molecules within the MFI framework is noncentrosymmetric, which leads to the SHG property.

In summary, by using a TPAOH nutrition supplemental method, a transparent and smooth larger zeolite MFI single crystal 3 × 1.5 × 1.5 $mm^3$ in size was synthesized. After carefully calcination, the MFI single crystal still kept its good qualification. PNA-encapsulated zeolite MFI single crystal was prepared by physical vapor deposition. The experimental results

showed that the PNA molecular monomers were encapsulated in the channels of MFI, and the PNA/MFI single crystal presents significant SHG property. The most suitable configuration of PNA/MFI simulated by the Monte Carlo method indicated that the structure of the PNA organic molecule did not possess a symmetric center, which led to the SHG from PNA/MFI single crystal. Such a novel SHG-active functional material PNA/MFI single crystal would potentially be used in the application of NLO materials and optoelectronic microdevices.

**Acknowledgment.** We are grateful to the financial support of the State Basic Research Project (G2000077507) and the National Natural Science Foundation of China (Grant No. 29873017 and 20101004). We also thank Professor Osamu Terasaki (Tohoku University), Professor Ying Mu, Dr. Qingxin Yang and Daming Zhang (Phys. Department JLU) for their helpful discussion.

## References and Notes

(1) Dalton, L. R.; Harper, A. W.; Wu, B.; Ghosn, R.; Laquindanum, J.; Liang, Z.; Hubbel, A.; Xu, C. *Adv. Mater.* **1995**, *7*, 519.

(2) Dalton, L. R.; Harper, A. W.; Ghosn, R.; Steier, W. H.; Ziari, M.; Fetterman, H.; Shi, Y.; Mustacich, R. V.; Jen, A. K. Y.; Shea, K. J. *Chem. Mater.* **1995**, *7*, 1060.

(3) Marks, T. J.; Ratner, M. A. *Angew. Chem., Int. Ed. Engl.* **1995**, *34*, 155.

(4) Moerner, W. E.; Silence, S. M. *Chem. Rev.* **1994**, *94*, 127.

(5) Katz, H. E.; Wilson, W. L.; Scheller, G. *J. Am. Chem. Soc.* **1994**, *116*, 6636.

(6) Agullo-Lopez, F.; Cabrera, J. M.; Agullo-Rueda, F. *Electrooptics: Phenomena, Materials and Applications*; Acdemic Press: New York, 1994.

(7) Zyss, J. *Molecular Nonlinear Optics: Materials, Physics, and Devices*; Academic Press: New York, 1993.

(8) Wyckoff, R. W. *Crystal Structures*; Wiley: New York, 1969; Vol. 6, p 120.

(9) Kagawa, H.; Sagawa, M.; Hamada, T.; Kakuta, A.; Kaji, M.; Nakayama, H.; Ishii, K. *Chem. Mater.* **1996**, *8*, 2622.

(10) Evans, O. R.; Lin, W. *Chem. Mater.* **2001**, *13*, 2705.

(11) Lin, W.; Lin, W.; Wong, G. K.; Marks, T. J. *J. Am. Chem. Soc.* **1996**, *118*, 8034.

(12) Ihlein, G.; Schuth, F.; Krauss, O.; Vietze, U.; Laeri, F. *Adv. Mater.* **1998**, *10*, 1117.

(13) Forrest, S. R. *Nature* **1999**, *397*, 294.

(14) Ozin, G. A.; Ozkar, S. *Chem. Mater.* **1992**, *4*, 511.

(15) Zhang, Z.; Dai, S.; Hunt, R. D.; Wei, Y.; Qiu, S. *Adv. Mater.* **2001**, *13*, 45.

(16) Ilemoto, Y.; Nakano, T.; Nozue, Y.; Terasaki, O.; Qiu, S. *Mater. Sci. Eng. B* **1997**, *48*, 116.

(17) Li, X.; Shao, C.; Qiu, S.; Xiao, F.; Zheng, W.; Ying, P.; Terasaki, O. *Micropor. Mesopor. Mater.* **2000**, *40*, 263.

(18) Gao, F.; Zhu, G.; Li, X.; Li, B.; Terasaki, O.; Qiu, S. *J. Phys. Chem. B* **2001**, *105*, 12708.

(19) Gener, I.; Ginestet, G.; Buntinx, G.; Bremard, C. *Phys. Chem. Chem. Phys.* **2000**, *2*, 1855.

(20) Bates, S. P.; van Well, W. J. M.; van Santen, R. A.; Smit, B. *J. Phys. Chem.* **1996**, *100*, 17573.

(21) Channon, Y. M.; Catlow, C. R. A.; Gorman, A. M.; Jackson, R. A. *J. Phys. Chem. B* **1998**, *102*, 4045.

(22) de vos Burchart, E.; van Bekkum, H.; van de Graaf, B.; Vogt, E. T. C. *J. Chem. Soc., Faraday Trans.* **1992**, *88*, 2761.

(23) Mayc, S. L.; Olafson, B. D.; Goddard, W. A. *J. Phys. Chem.* **1990**, *94*, 8897.

(24) Metropolis, N.; Rosenbluth, A. W.; Rosenbluth, M. N.; Teller, A. H.; Teller, T. *J. Chem. Phys.* **1953**, *21*, 1085.

(25) Lin-Vien, D.; Colthup, N. B.; Fateley, W. G.; Grasselli, J. G. *The Handbook of Infrared and Raman Characteristic Frequencies of Organic Molecules*; Academic Press, Harcourt Brace Jovanovich: New York, 1991.

(26) *Sadtler Standard Spectra: Raman Spectra*; Sadtler Research Laboratories: Philadelphia, PA, 1973.

(27) Dollish, F. R.; Fateley, W. G.; Bentley, F. F. *Characteristics Ramam Frenquencies of Organic Compounds*; Wiley-Interscience Publication: New York, 1973.